Substoichiometric Conversion of Biomass and Solid Wastes to Energy in Packed Beds

Yao Bin Yang, Vida Nasserzadeh Sharifi, and Jim Swithenbank
Sheffield University Waste Incineration Centre (SUWIC), Dept. of Chemical and Process Engineering, Sheffield University, Mappin Street, Sheffield, S1 3JD, U.K.

DOI 10.1002/aic.10646
Published online September 15, 2005 in Wiley InterScience (www.interscience.wiley.com).

Biomass and municipal solid wastes are two of the sustainable energy resources. Countercurrent, substoichiometric conversion of these fuels into energy in packed beds has the benefits of lower tar and dust carryover in flue gases, and therefore gas-treatment procedures can be simplified and the running cost is reduced. In this paper, mathematical simulation is performed on a large-scale plant furnace for both municipal solid wastes and biomass fuels in a range of operating conditions. The temperature profile inside the moving packed bed of the same system was measured by an in situ electronic device for the baseline case to partially validate the simulation results. Mathematical simulation indicates that by using variable grate speed to obtain constant bed height, a typical moving-bed furnace can achieve over 99% of conversion efficiency with only 40–50% of the normal primary air supply, without loss in throughput; the char conversion rate is significantly lower than the devolatilization rate in the bed and the char conversion process occupies over half of the total bed length, whereas fuel devolatilization occupies only one-third or more of the bed length. © 2005 American Institute of Chemical Engineers *AIChE J,* 52: 809–817, 2006

Keywords: solid wastes, biomass, gasification, packed-bed, incineration, numerical modeling

Introduction

Sustainable development requires sustainable energy resources. The world biomass resources have the potential to provide 10–14% of the global primary energy, the fourth largest following coal, oil, and natural gas. It is renewable and produces no net CO_2 emission when converted to energy, thus having only a minimal effect on the environment. Another type of sustainable energy resources is municipal solid wastes (MSWs) or house refuse. MSWs generated in the United Kingdom amount to 30 million tons per year.[1] The available energy from these wastes could produce 2000 MW electricity and 6000 MW heat, equal to one major power station, that is, about 10% of UK power. A large proportion of MSWs is biomass or biomass-originated materials and the conversion of MSWs to energy produces only a negligible fraction of net CO_2 compared to fossil fuels.

The most common technology for converting biomass and MSWs to energy is in packed-bed reactors. If a fixed bed is used, a batch of fuel is placed on a grate to form a bed and air supplied to the fuel from underneath. Ignition starts at the bed top. A flame front is formed and then travels down the bed against the direction of air flow. This is called *countercurrent conversion* (Figure 1a). Moving beds are used for industrial scales and work in a way the similar to that of fixed beds, except that the fuel is fed continuously from an entrance, carried forward by a moving grate as the conversion reactions proceed and exits at the ash port.

Most bed reactors in waste-to-energy (WTE) plants operate under superstoichiometric conditions. Primary air enters the bed in an excessive amount so that the air supply is more than the minimum required to burn the fuels completely. Secondary

Correspondence concerning this article should be addressed to Y. B. Yang at y.b.yang@Sheffield.ac.uk.

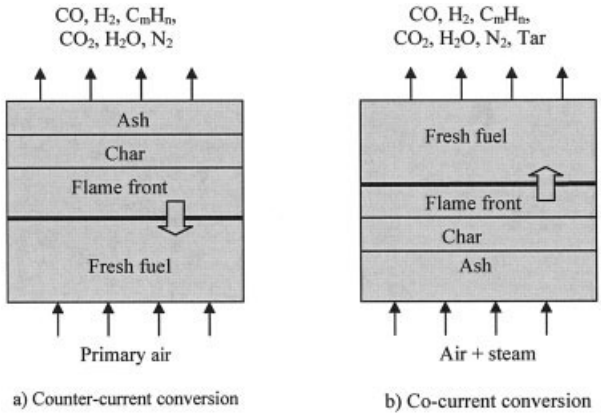

Figure 1. Countercurrent and cocurrent packed-bed conversion of solid fuels.

(a) Countercurrent conversion; (b) cocurrent conversion.

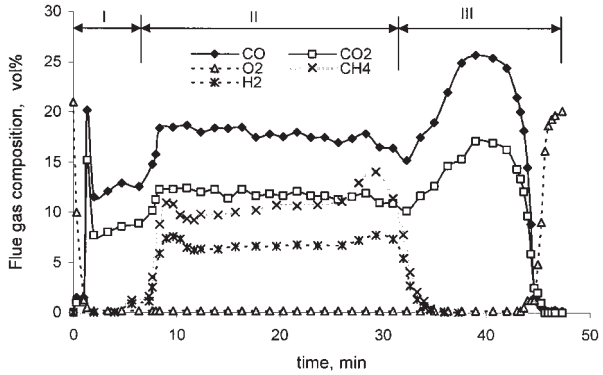

Figure 2. Composition of flue gases of a wood fuel at primary air velocity 0.1 kg m^{-2} s^{-1} in a fixed bed of initial height 400 mm.

I: ignition; II: devolatilization and substoichiometric combustion of volatile gases; III: char gasification.

air is further added to the combustion products (flue gases exiting the bed) downstream to ensure any remaining unburned species are consumed.

For waste incineration, this kind of practice attracts unfavorable opinions from the general public. Despite the fact that all modern waste incineration plants fully meet the environmental standards, the building of new plants meets stiff opposition from some political groups. At the same time, a large proportion of MSWs is being dumped to many landfill sites, which require year-round management, produce methane (an important greenhouse gas) emission to the atmosphere, and impose a risk to underground water.

Gasification provides a more acceptable alternative. Gasification was historically defined as converting solid-phase fuels into combustible gaseous products, which can then be either used as gas fuels or synthesized into other chemicals. In principle, gasification is a substoichiometric conversion of solids, using air with the addition of small amounts of steam as the oxidizers. The traditional gasification design in packed beds is *cocurrent*, that is, the flame front propagates in the direction of the oxidizer flow (Figure 1b). This approach results in high conversion rates and high heating values of the gaseous products. The disadvantage, however, is the high level of tar in the products, which can deposit on walls and block small openings in the equipment. The building and operation of cocurrent packed-bed gasifiers are also costly.

On the other hand, the countercurrent packed-bed conversion of solid fuels can be operated in substoichiometric conditions. It is one of the nondirect burning technologies and similar to the cocurrent gasification, producing CO, H_2, CH_4, and other hydrocarbons from the solids by harnessing the low velocity of primary air. These combustible gases are then burned in a separate combustion chamber with well-controlled environment. Compared to traditional gasification, the tar concentration in the over-bed flue gases is much lower because the hot char layer above the flame front helps to crack the tar from the pyrolysis process.

The greatest advantage of substoichiometric countercurrent conversion is that most of the existing WTE plants or new designs can adapt easily to this technique without much modification of the hardware. Compared to waste incineration, this technique has lower dust carryover in the flue gases, lower bed temperature (and therefore lower NO_x formation in the bed), and simplified gas-treatment procedures and running costs, among other benefits.

In this article, substoichiometric countercurrent conversion of MSWs and biomass fuels is explored. For moving beds in industrial scale, mathematical modeling and a numerical method are used. Results are presented in terms of detailed burning characteristics such as mass-loss rate, temperature profile, gas composition, and conversion efficiency. The effects of operating parameters are discussed.

Substoichiometric Conversion of Biomass and Simulated MSWs in Fixed Beds

A number of experiments and modeling work have been done with biomass and simulated MSWs in the past. Gort[2] carried out systematic experiments in packed beds firing both solid wastes and biomass and the effect of operating properties including superficial air velocity, moisture, fuel volatile content, and particle size was discussed. Rönnbäck et al.[3] tested wood chips and wood pellets in a wide range of primary air mass flows. Friberg and Blasiak[4] fired the same wood material in chips, pellets, and logs and measured the conversion mass flux and off-gas composition. Yang et al.[5] investigated the

Table 1. Typical Fuel Analysis for Biomass (Wheat Straw) and MSWs

	Proximate Analysis (wt %)				Ultimate Analysis (wt %, daf)						
	Moisture	Volatile Matter	Fixed Carbon	Ash	C	H	O	N	S	Other	LCV (MJ/kg)
Biomass	15.2	63.5	15.2	6.1	49.8	6.6	41.2	0.67	0.35	1.38	15.0
MSWs	28	40.8	7.2	24	49.6	7.3	38.3	1.5	0.4	2.9	9.05

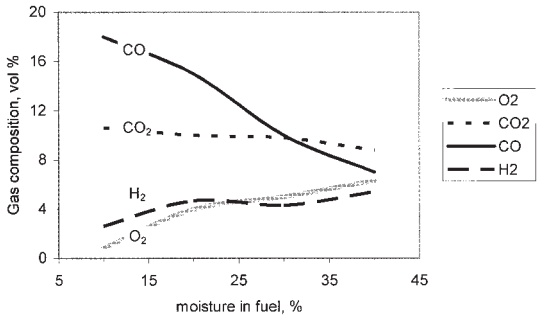

Figure 3. Gas composition at the bed top vs. fuel moisture at primary air velocity 0.13 kg m^{-2} s^{-1}.

Data are extracted from Yang et al.[13]

combined effect of fuel moisture content and primary air flow rate based on both experiments and mathematical modeling. Other important works include Thunman and Leckner,[6] Saastamoinen et al.,[7] Peters,[8] Yang et al.,[9,10] and Van et al.[11]

Figure 2 shows the composition of flue gases in a series of tests and modeling work carried out recently on a bench-top fixed-bed reactor firing pinewood cubes of 10 mm.[12] The reactor was 0.2 m in inner diameter and 2.0 m in total height. Temperature and gas species were measured as a function of reaction time, which can be converted to traveling distance along the bed length for a large-scale moving-bed furnace, if the moving velocity of the grate is given. Thus results on the bench-top fixed bed can be related to the operation of a large-scale moving-bed furnace. The wood contains 5.9% moisture, 80.5% volatile matter, 1.1% ash, and 12.7% fixed carbon. The conversion process is roughly divided into three stages: the ignition stage, primary conversion stage, and char gasification stage.

Although over 70% of the mass in MSWs is biomass, properties of MSWs and biomass fuels differ only modestly, largely with respect to the moisture and ash levels. Table 1 shows typical fuel analysis of biomass and MSWs. Our earlier study[13] showed that moisture content in fuel plays a crucial role in determining the conversion characteristics. Figure 3 shows the flue-gas composition as a function of moisture content in

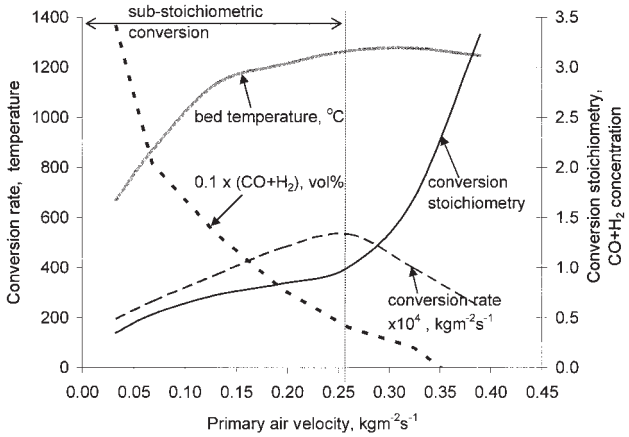

Figure 4. Effects of primary air velocity in fixed-bed countercurrent conversion.

Fuel moisture 20 wt%; data are extracted from Yang et al.[13]

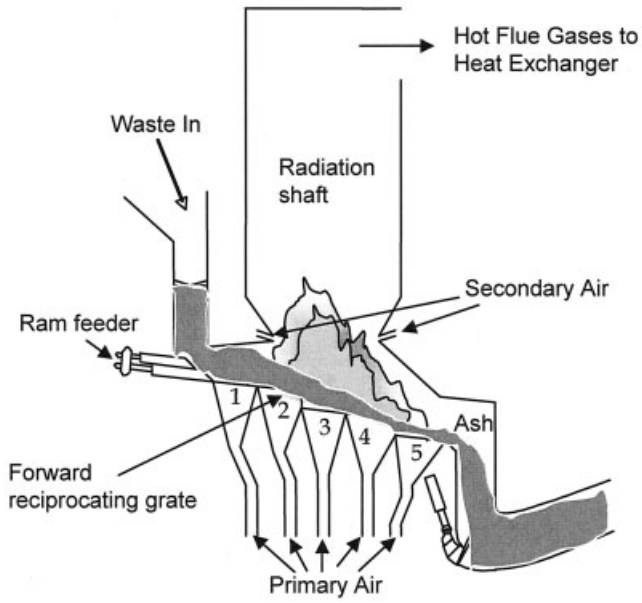

Figure 5. Furnace section of a large waste-to-energy plant.

fuel. As moisture increases, flue-gas CO diminishes whereas O_2 increases, although there is less effect on CO_2 and H_2 concentrations. Judging from this, MSWs would produce less CO than biomass under the same conditions.

Another influential parameter is the primary air velocity. Figure 4 shows the extracted results from Yang et al.[13] obtained for a fixed-bed reactor burning simulated wastes at 20% moisture. In the figure the conversion rate is the rate at which the solid fuel is converted from the solid phase to the gas phase by moisture evaporation, devolatilization, and char burn-out. *Conversion stoichiometry* is defined as the ratio of actual air supply to the bed to the theoretical air flow required for complete combustion, that is, the residual combustible species in the flue gases is zero. At a fixed air flow rate, the higher the conversion rate, the lower the conversion stoichiometry. By reducing the primary air-flow rate through the grate of a packed-bed system, operation of the bed is shifted from superstoichiometric mode (conversion stoichiometry > 1.0) to substoichiometric mode (conversion stoichiometry < 1.0). Traditionally, superstoichiometric mode is called *combustion*, whereas substoichiometric mode is known as *gasification*. Figure 4 demonstrates that as the primary air velocity decreases to <0.25 kg m^{-2} s^{-1}, operation of the bed becomes substoichiometric. The concentrations of the major combustible gaseous species ($CO + H_2$) exiting the bed top increase and the bed temperature decreases.

The major disadvantages, however, are reduced conversion rate and possibly higher carbon in the ash at the bed exit.

Conversion of Biomass and MSWs in Industrial-Scale Moving Beds

In a fixed bed, the conversion process is a function of time; in a moving bed, the conversion process is a function of position along the bed length. There are two extra features for the moving-bed conversion, however: the grate-moving mechanism causes mixing between fresh fuel particles and burning

Table 2. Summary of Reactions and Transport Equations Used in the Mathematical Simulation

		Reference
Process Rate Equations		
Moisture evaporation	$R_m = A_p h_s (C_{w,s} - C_{w,g})$ when $T_s < 100°C$	Yang et al.[16]
	$R_m = \dfrac{A_p\lfloor h_s'(T_g - T_s) + \varepsilon_s \sigma_b (T_{env}^4 - T_s^4)\rfloor}{H_{evp}}$ when $T_s = 100°C$	
Devolatilization	$R_v = (1-\phi)\rho_s k_v (v_\infty - v) \qquad k_v = A_v \exp\left(-\dfrac{E_v}{RT_s}\right)$	Badzioch[18]
Combustion of volatiles	$C_mH_n + \dfrac{m}{2}O_2 \rightarrow m\text{CO} + \dfrac{n}{2}H_2 \qquad R_{C_mH_n} = 59.8\, T_g{}^{0.3} \exp\left(\dfrac{-12200}{T_g}\right) C_{C_mH_n}^{0.5} C_{O_2}$	Siminski et al.[19]
	$\text{CO} + \dfrac{1}{2}O_2 \rightarrow CO_2 \qquad R_{CO} = 1.3 \times 10^{11} \exp\left(\dfrac{-62700}{T_g}\right) C_{CO} C_{H_2O}^{0.5} C_{O_2}^{0.5}$	Howard et al.[20]
	$H_2 + \dfrac{1}{2}O_2 \rightarrow H_2O \qquad R_{H_2} = 3.9 \times 10^{17} \exp\left(\dfrac{-20500}{T_g}\right) C_{H_2}^{0.85} C_{O_2}^{1.42}$	Hautman et al.[21]
	$R_{mix} = C_{mix}\rho_g \left[150\dfrac{D_g(1-\phi)^{2/3}}{d_p^2\phi} + 1.75\dfrac{V_g(1-\phi)^{1/3}}{d_p\phi}\right] \min\left[\dfrac{C_{fuel}}{S_{fuel}}, \dfrac{C_{O_2}}{S_{O_2}}\right] \qquad R = \min[R_{kinetic}, R_{mix}]$	Yang et al.[16]
Char gasification	$C(s) + \alpha O_2 \rightarrow 2(1-\alpha)\text{CO} + (2\alpha - 1)CO_2 \qquad \dfrac{\text{CO}}{CO_2} = 2500 \exp\left(-\dfrac{6420}{T}\right)$	Arthur[23]
	$R_C = A_P C_{O_2} \Big/ \left(\dfrac{1}{k_r} + \dfrac{1}{k_d}\right) \qquad k_r = A_r \exp\left(-\dfrac{E_r}{RT_s}\right)$	Gray et al.[24] Field[25]
Gas-Phase Conservation Equations		
Continuity	$\dfrac{\partial(\rho_g\phi)}{\partial t} + \dfrac{\partial(\rho_g U_g \phi)}{\partial x} + \dfrac{\partial(\rho_g V_g \phi)}{\partial y} = S_{sg}$	Peters[26]
x-Momentum	$\dfrac{\partial(\rho_g U_g \phi)}{\partial t} + \dfrac{\partial(\rho_g U_g U_g \phi)}{\partial x} + \dfrac{\partial(\rho_g U_g V_g \phi)}{\partial y} = -\dfrac{\partial p_g}{\partial x} + F(U_g)$	
y-Momentum	$\dfrac{\partial(\rho_g V_g \phi)}{\partial t} + \dfrac{\partial(\rho_g V_g U_g \phi)}{\partial x} + \dfrac{\partial(\rho_g V_g V_g \phi)}{\partial y} = -\dfrac{\partial p_g}{\partial y} + F(V_g)$	
Species	$\dfrac{\partial(\rho_g Y_{i,g}\phi)}{\partial t} + \dfrac{\partial(\rho_g U_g Y_{i,g}\phi)}{\partial x} + \dfrac{\partial(\rho_g V_b Y_{i,g}\phi)}{\partial y} = \dfrac{\partial}{\partial x}\left(D_{ig}\dfrac{\partial(\rho_g Y_{i,g}\phi)}{\partial x}\right) + \dfrac{\partial}{\partial y}\left(D_{ig}\dfrac{\partial(\rho_g Y_{i,g}\phi)}{\partial y}\right) + S_{Y_{i,g}}$	
	$D_{ig} = E^0 + 0.5 d_P \lvert V_g \rvert$	Wakao and Kaguei[27]
Energy	$\dfrac{\partial(\rho_g H_g \phi)}{\partial t} + \dfrac{\partial(\rho_g U_g H_g \phi)}{\partial x} + \dfrac{\partial(\rho_g V_g H_g \phi)}{\partial y} = \dfrac{\partial}{\partial x}\left(\lambda_s \dfrac{\partial T_g}{\partial x}\right) + \dfrac{\partial}{\partial y}\left(\lambda_s \dfrac{\partial T_g}{\partial y}\right) + Q_h$	Peters[26]
	$\lambda_g = \lambda^0 + 0.5 d_P \lvert V_g \rvert \rho_g C_{pg}$	Wakao and Kaguei[27]
Solid-Phase Conservation Equations		
Continuity	$\dfrac{\partial((1-\phi)\rho_s)}{\partial t} + \dfrac{\partial((1-\phi)\rho_s U_s)}{\partial x} + \dfrac{\partial((1-\phi)\rho_s V_s)}{\partial y} = -S_{sg} \qquad U_s = f(x)$, predefined	Yang et al.[10]
Species	$\dfrac{\partial((1-\phi)\rho_s Y_{i,s})}{\partial t} + \dfrac{\partial((1-\phi)\rho_s U_s Y_{i,s})}{\partial x} + \dfrac{\partial((1-\phi)\rho_s V_s Y_{i,s})}{\partial y}$ $+ \dfrac{\partial}{\partial x}\left(D_s \dfrac{\partial((1-\phi)\rho_s Y_{i,s})}{\partial x}\right) + \dfrac{\partial}{\partial y}\left(D_s \dfrac{\partial((1-\phi)\rho_s Y_{i,s})}{\partial y}\right) - S_{Y_{i,s}}$	
Energy	$\dfrac{\partial((1-\phi)\rho_s H_s)}{\partial t} + \dfrac{\partial((1-\phi)\rho_s U_s H_s)}{\partial x} + \dfrac{\partial((1-\phi)\rho_s V_s H_s)}{\partial y} = \dfrac{\partial}{\partial x}\left(\lambda_s \dfrac{\partial T_s}{\partial x}\right)$ $+ \dfrac{\partial}{\partial y}\left(\lambda_s \dfrac{\partial T_s}{\partial y}\right) + \dfrac{\partial q_{rx}}{\partial x} + \dfrac{\partial q_{ry}}{\partial y} + Q_{sh}$	
Radiation Heat Transfer		
	$\dfrac{dI_{xi}^{\pm}}{dx_i} = -(k_a + k_s) I_{xi}^{\pm} + \dfrac{1}{2N} k_a E_b + \dfrac{1}{2N} k_s \sum_{i=1}^{N} (I_{xi}^{+} + I_{xi}^{-}),\ i = 1,N$	Gosman and Lockwood[29]
	$k_s = 0 \qquad k_a = -\dfrac{1}{d_p}\ln(\phi)$	Shin and Choi[28]

Table 3. Source Terms in the Conversation Equations

Conversation Equation	Source Term
Solid and gas continuity	$S_{sg} = R_m + R_v + R_C$
C_mH_n	$S_{y1,g} = \min(R_{C_mH_n}, R_{mix,C_mH_n})$
CO	$S_{y2,g} = \min(R_{H_2}, R_{mix,H_2})$
H_2	$S_{y3,g} = \min(R_{H_2}, R_{mix,H_2})$
Moisture in fuel	$S_{y1,s} = -R_m$
Volatile in solid phase	$S_{y2,s} = -R_v$
Fixed carbon in fuel	$S_{y3,s} = -R_C$
Ash	$S_{y4,s} = 0$

hot particles, enhancing the conversion rate[14]; the speed of the grate can be varied along the bed length so that the desired bed-height profile can be achieved. Figure 5 illustrates the furnace section of a typical WTE plant. The furnace system includes the stock hopper to put the waste in, a ram feeder pushing the waste onto the bed, a forward-reciprocating grate moving the burned waste to the ash port, secondary air injection burning any remaining unburned species from the bed, and radiation shaft cooling down the flue gases to around 850°C. Primary air is supplied to the underside of the grate in five separate zones, each with a different primary air flow rate. The grate has a total length of nearly 11 m and a width of about 6 m with a capacity burning 23 tons of MSWs per hour and 25 MW electricity output.

Experiments on full-scale moving-bed furnaces are extremely difficult and costly. Measurements are limited by the few access ports and the size of the furnace geometry. The measured data were often lacking in details, fluctuating and impeded by operational irregularities.[9,15] Mathematical simulation, on the other hand, provides detailed analysis of conversion characteristics, including conversion rate, temperature profile, gaseous species concentration, and conversion efficiency, which are impossible to obtain by conventional experimental means. In the following sections, superstoichiometric conversion (combustion mode), substoichiometric conversion (gasification mode), and constant bed-height operation mode are to be simulated mathematically based on the design of this typical plant. Temperature measurement inside the moving bed was also carried out using an in situ electronic device. Different operating conditions are compared and discussed.

Transport equations and reactions for the mathematical simulation

The moving bed is viewed as a continuous porous medium consisting of solid and gas phases. The solid phase has four components: moisture, volatile matter, fixed carbon, and inert ash. The gas phase has different species, including O_2, N_2, CO, CO_2, C_mH_n, H_2, and H_2O. The bed is ignited from the top layer and the flame front travels down the bed until reaching the bottom (grate). As the flame front passes by, the solid phase successively undergoes moisture evaporation, devolatilization, and char gasification. For the gas phase, the cohort of released volatiles (mainly CO, C_mH_n, H_2, and some H_2O and CO_2 as well) mixes and reacts with the primary air from beneath the grate in the many voids inside the bed. Propagation of the flame front is mainly driven by radiation penetration in the bed, through the voids between the particles. Tables 2 and 3 summarize the reaction rates and transport equations for both solid and gas phases. More detailed explanation of the models can be found in the work of Yang et al.[9,16] The model assumes uniform distribution of parameters across the bed width and calculation is carried out in the bed height and length directions (2D simulation).

Numerical simulation using the above equations and process rates are carried out for different operating conditions illustrated in Table 4. There are two different timescales for the reactions. For solid-phase reactions including volatile release and char gasification, the timescale is large; for gas-phase reactions (combustion of CO, C_mH_n, and H_2), the timescale is significantly small. To obtain numerical stability and accuracy of the simulation, the conservation equations of the solid and gas phases are solved separately. Besides, the SIMPLE algorithm—used by many successful computational fluid dynamics (CFD) codes for fluid flow, heat transfer, and combustion—was used to solve the equations.

Numerical simulation and temperature measurements at standard operating conditions

The standard operation of this plant is in superstoichiometric conversion mode for the bed where the equivalent ratio of the primary air supply to the fuel feeding rate is around 1.25 (Case 0 in Table 4). The total air-to-fuel equivalent ratio for the furnace is 1.8 (including the secondary air). Distributions of primary air among sections 1 to 5 are 15, 30, 35, 15, and 5%, respectively. Figure 6 shows the simulation results for species concentrations in the flue gases exiting the bed top and the fixed-carbon profile in the bed. It is seen that for the first 3 m along the bed length (starting from the fuel entrance), only H_2O is produced from moisture evaporation and O_2 remains around 18 vol % in the flue gases. This is followed by a sharp decline in O_2 and sharp increase in CO_2, indicating the fuel has been ignited. During the combustion period, CO and H_2 rise to around 3 vol % and C_mH_n rises first then slowly decreases to zero. H_2O is at an elevated level from both the fuel drying process and the burning of H_2 and hydrocarbon gases (C_mH_n) with O_2. At 7.5 m along the bed length, H_2O, C_mH_n, and H_2 fall to zero, indicating the completion of the devolatilization process. Further on, the char burning begins and there is gradual increasing of O_2 and decreasing of CO_2. The CO level is

Table 4. Simulated Moving-Bed Operating Conditions

No.	Fuel Type	Feeding Rate (tons h^{-1})	Primary Air Velocity ($kg/m^{-2}/s^{-1}$)		Conversion stoichiometry	Constant Bed Height
			Average	Peak		
0	MSWs	23.5	0.33	0.65	1.25	No
1	MSWs	23.5	0.16	0.32	0.6	No
2	MSWs	21.0	0.12	0.24	0.5	Yes
3	Biomass	23.5	0.16	0.32	0.40	No
4	Biomass	23.5	0.16	0.32	0.40	Yes

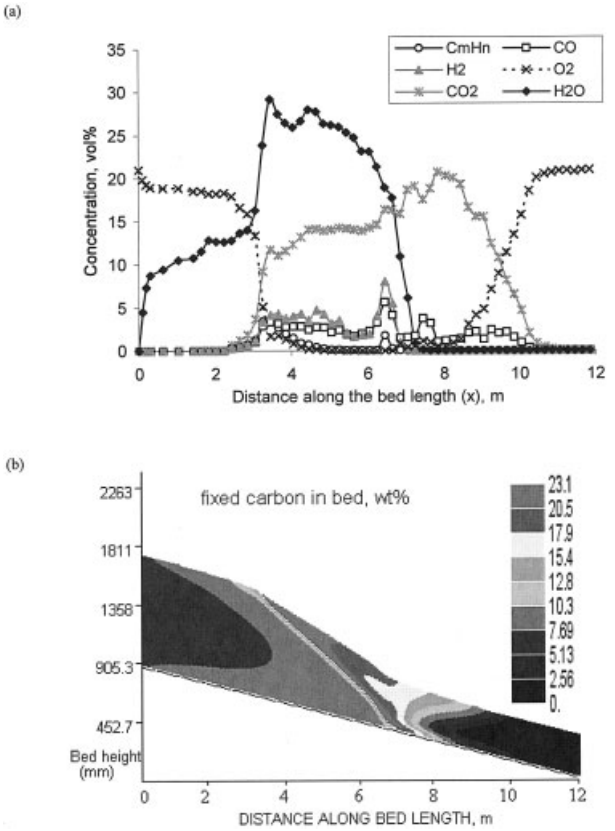

Figure 6. Simulation results for the standard conversion mode.

Case 0: MSWs, 100% baseline primary air, uniform bed speed, and decreasing bed height: (a) gas composition at the bed top; (b) fixed carbon profile in bed.

maintained at around 2 vol % during this period. The whole conversion process finishes at 10.5m from the fuel entrance, 1 m before the ash exit.

Figure 6b presents the fixed-carbon profile in the bed. With the conversion process proceeding, the fixed-carbon concentration in the solids increases from 7 wt % in the fresh fuel to a maximum of 23 wt % after all the local moisture and volatile matter are released. Then the fixed-carbon concentration begins to decrease at roughly 5 m along the bed length. The unburned carbon in the exit ash is around 1.5%.

For measurement inside the burning bed, a unique in-house prototype instrument (Figure 7) was used that can be introduced into the incinerator with the waste feed and tumbles along with the burning waste material while recording temperature and bed motion onto its thermally insulated electronic chip. This unique instrument, in the shape of a cylinder, contains thermally protected sensors and a miniature data logger. Before the experiment, the device was thrown into the feeding hopper and was mixed with and carried along by the fresh waste stream into the burning chamber. The device was later recovered manually at the transporting belt, which removes the ash from the furnace. The stored data on the memory chip were downloaded to a computer to be analyzed. Details of the electronic device are reported in the work of Yang et al.[17]

Figure 8 presents the measured temperature profile using the electronic device and the simulation results. There are three stages for the temperature variation along the bed length. The first stage covers the bed position from 4 to 7 m and the maximum bed temperature is 980°C (measured) and 1100°C (simulation). The second stage covers the bed from 7 to 9 m and the maximum bed temperature is 1300°C (measured) and 1370°C (simulation). The third stage runs from 9 m until the ash exit, during which the bed temperature gradually decreases from 1300 to 500°C. By combining the gas composition profile shown in Figure 6a and the temperature profile in Figure 8, it can be concluded that the first stage primarily constitutes devolatilization and gas burning process, whereas the second stage is mainly char burning. The third stage is the end of char burning, showing an increasing O_2 level in the flue gases.

Substoichiometric conversion of MSWs in an existing WTE plant

Temperature measurement inside the burning bed shows good agreement between the simulation and the actual working conditions. The numerical technique is thus further used to simulate the substoichiometric conversion of MSWs in an existing WTE plant. Two situations are simulated: Cases 1 and 2 and their operating conditions are shown in Table 4. For Case 1, the primary air flow rate is reduced to 45% of the original and the air-to-fuel stoichiometric ratio in bed is reduced from 1.25 to 0.55. The feeding rate remains unchanged. It is found that the carbon content in the final ash is 13% high and the thermal conversion efficiency is only 93%, below the official requirements for WTE plants. In Case 2, the feeding rate is reduced to 90% of the original load and the air-to-fuel equivalent ratio in the bed is set at 0.5. Moreover, the bed height is maintained constant during the conversion process by slowing down the grate speed as the conversion proceeds along the bed length. This ensures complete gasification of the char and thus an acceptable level of unburned carbon in exit ash.

Figure 9 presents the simulated results for the flue gas composition at substoichiometric conversion mode (Case 2). Compared to Figure 6a for the superstoichiometric conversion mode (Case 0), concentrations of the combustible species (CO, C_mH_n, H_2) in the bed-top flue gases are twice as high, whereas CO_2 concentration remains roughly the same during the pyrolysis stage after ignition. The greatest difference is in the char gasification stage starting from 6.5 m along the bed length. The CO level is 17% high, compared to only 2% for the standard operating mode (Case 0), which arises from a much thicker

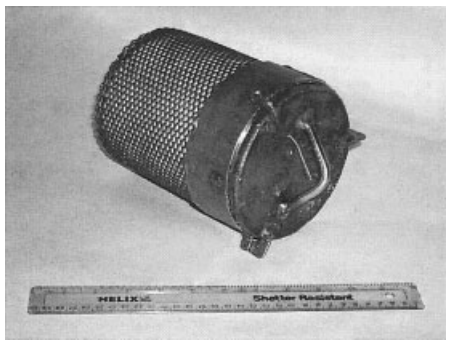

Figure 7. Photographs of the electronic device used for temperature measurement within the burning bed.

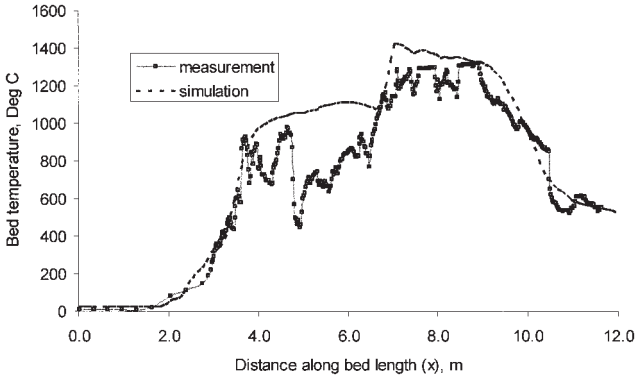

Figure 8. Comparison between the measured temperature profile using the electronic device and the simulation results.

Case 0: MSWs, 100% baseline primary air, uniform bed speed, and decreasing bed height.

layer of char in the latter part of the bed, which in trun enhances the gasification efficiency. At standard operating conditions, the latter part of the bed is thin and the air velocity is high, thus favoring superstoichiometric conversion of the char.

Calculation indicates that the unburned carbon in ash is $<1.5\%$.

Substoichiometric conversion of biomass in the moving bed

Generally, biomass differs from MSWs in moisture and ash levels, the former being drier and having less inert materials (ash). It is very interesting to investigate the biomass conversion on the same moving grate as in the cases of MSW conversion. Two cases (3 and 4) have been simulated and their operating conditions are shown in Table 4. The same fuel feeding rate is used and the conversion stoichiometry in the bed is set at 0.4.

Numerical simulation indicates that when using the uniform grate speed and thus a decreasing bed-height profile (Case 3), the carbon concentration in the final ash is around 50% and the thermal conversion efficiency is 91%, which do not meet the standards set by the environmental agencies. However, when

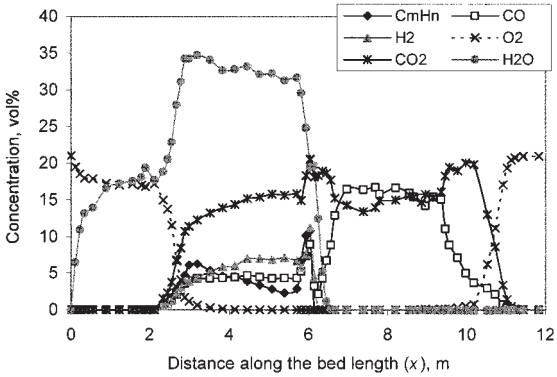

Figure 9. Flue gas composition at the bed top for substoichiometric conversion mode.

Case 2: MSWs, 36% baseline primary air, variable bed speed, and constant bed height.

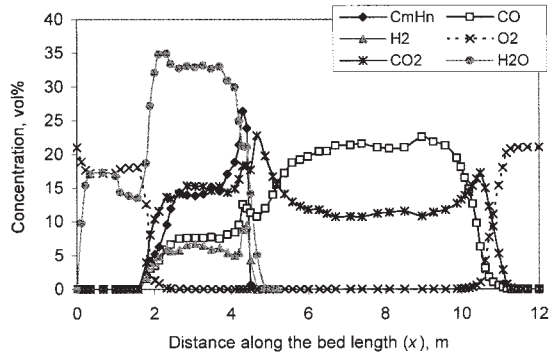

Figure 10. Flue gas composition at the bed top for substoichiometric conversion mode.

Case 4: biomass fuel, 50% baseline primary air, variable bed speed, and constant bed height.

using the variable-grate-speed mode and thus the constant bed-height profile (Case 4), the final carbon in ash is reduced to $<1.0\%$ and the conversion efficiency is $>99\%$. Figure 10 presents the species concentration in the flue gases exiting the bed as a function of position along the bed length. Compared to Figure 9 for the conversion of MSWs, O_2 drops to zero at 2 m from the fuel entrance, indicating the bed is being ignited. The ignition distance is 1 m shorter than that for MSWs where the ignition starts at 3 m from the fuel entrance. After the ignition, the concentrations of C_mH_n, CO, and H_2 increase to 15, 7, and 6 vol %, respectively, and these are compared to 4, 4, and 5%, correspondingly shown in Figure 9 for conversion of MSWs. As the moisture evaporation front reaches the bed bottom, the concentrations of C_mH_n and H_2 rise to staggeringly high levels of 25 and 10%, respectively, before falling sharply to zero. The char gasification reaction follows, featuring a higher level of CO in the flue gases than that for the case of MSWs (22 vs. 17%). Two meters away from the ash exit, the char conversion changes from gasification mode to combustion mode, indicated by the rising level of O_2 in the flue gases. The whole conversion process completes at the 11 m position.

Discussion

The preceding numerical simulations demonstrate that countercurrent, substoichiometric conversion of both MSWs and biomass in moving-grate systems is possible without loss in throughput or conversion efficiency. Comparison of the bed-top species composition profiles under substoichiometric conversion mode (Figures 2, 9, and 10) shows the same trend between a fixed bed and a moving bed, that is, a stage of devolatilization and substoichiometric burning of volatile gases with high concentrations of hydrocarbon, CO, and H_2 in the flue gases, followed by a stage of char gasification where the CO level can reach as high as 22%. This is in contrast to the combustion mode on the moving grate (Figure 6a) where these two stages operate at near-stoichiometric levels and very low concentrations of combustible gases exist in the flue gases from the bed top.

However, using uniform-grate speed as in the standard operation where the bed height decreases as the conversion process proceeds, substoichiometric conversion of both MSWs and biomass results in unacceptably high levels of unconverted

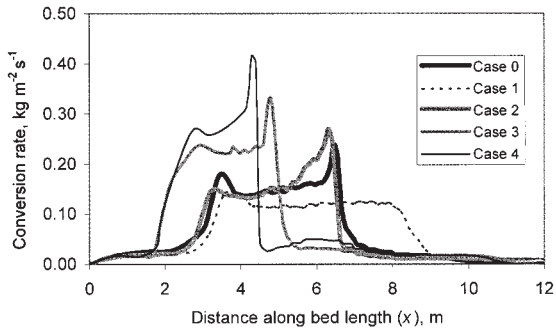

Figure 11. Fuel conversion rate as a function of position along the bed length.

Case 0: MSWs, full load, 100% baseline primary air, decreasing bed height; Case 1: MSWs, full load, 50% baseline primary air, decreasing bed height; Case 2: MSWs, 90% load, 36% baseline primary air, constant bed height; Case 3: biomass, full load, 100% baseline primary air, decreasing bed height; Case 4: biomass, full load, 50% baseline primary air, constant bed height.

carbon in the exit ash (Cases 1 and 3). Figure 11 demonstrates the conversion rate as a function of position along the bed length and it is seen that char conversion occupies from 1/2 to 2/3 of the total bed length, whereas fuel devolatilization occupies only 1/3 to 2/5 of the bed length. Char conversion is significantly slower and requires a high temperature level. The process is also less affected by particle mixing in the bed.[14]

Figure 11 also shows that biomass fuel has a longer period of char conversion than that of MSWs, which is attributed to 70% of carbon in the char formed from biomass vs. only 23% of carbon in the char formed from MSWs. By using variable grate speed to maintain a constant bed height, the residence time of the formed char in the bed extends to 90 min for MSWs (Case 2) and 180 min for biomass (Case 4), that is, two and three times, respectively, the char residence time obtained in standard operations (Cases 1 and 3), according to simulation.

The averaged devolatilization rate of biomass is twice as high as that for MSWs. This results from less moisture and ash content in, and thus higher heating value of, biomass fuel. Figure 11 confirms that the ignition position with biomass is 1 m shorter than that with MSWs, consistent with previous conclusions based on the species composition profile in the flue gases.

The benefits of substoichiometric conversion in a moving bed are obvious. Table 4 shows that the average primary air velocity diminishes from 0.33 kg m^{-2} s^{-1} in standard operation to 0.12–0.16 kg m^{-2} s^{-1} in the substoichiometric mode and the peak velocity falls from 0.65 to 0.24–0.32 kg m^{-2} s^{-1}. This substantially reduces the dust carryover in the flue gases and thus the particle (ash) deposition on the downstream heat exchanger surfaces. The workload of the cyclone dust collector and that of bad filters are also reduced. Moreover, the substoichiometric environment inside the bed prevents NO_x formation in the gaseous phase.

Conclusions

In this study, both fixed-bed and moving-bed substoichiometric conversions of municipal solid wastes and as well as biomass fuel have been investigated using mathematical simulation. Experimental measurements in a large-scale waste-to-energy furnace were also carried out using an in situ electronic device. The main conclusions are:

(1) Countercurrent, substoichiometric conversion of both municipal solid wastes and biomass in moving-grate systems is possible without loss in throughput or conversion efficiency.

(2) By using variable grate speed to obtain constant bed height, a typical moving-bed furnace can achieve >99% of conversion efficiency with only 40–50% of the normal primary air supply, substantially reducing dust carryover in the flue gases. The reducing environment inside the bed also prevents NO_x formation in the gaseous phase.

(3) Char conversion rate is significantly lower than the devolatilization rate and the char conversion process occupies >1/2 of the total bed length, whereas fuel devolatilization occupies only around 1/3 of the bed length.

(4) The averaged devolatilization rate of biomass is twice as high as that for municipal solid wastes as a result of less moisture and ash contents. Biomass fuel also requires a shorter distance to be ignited.

Acknowledgments

The authors thank the UK Engineering and Physical Sciences Research Council (EPSRC) for the financial support of this project.

Notation

A = particle surface area, m^2 m^{-3}
A_r = preexponent factor in char burning rate, kg m^{-2} s^{-1}
A_v = preexponent factor in devolatilization rate, s^{-1}
C = constant; molar fractions of species
C_{fuel} = fuel concentration, kg m^{-3}
C_{pg} = specific heat capacity of the gas mixture, J kg^{-1} K^{-1}
C_{mix} = mixing-rate constant, 0.5
$C_{w,g}$ = moisture mass fraction in the gas phase
$C_{w,s}$ = moisture mass fraction at the solid surface
D_{ig} = dispersion coefficients of the species Y_i, m^2 s^{-1}
d_p = particle diameter, m
E_b = black body emission, W m^{-2}
E_r = activation energy in char burning rate, J kmol^{-1}
E_v = activation energy in devolatilization rate, J kmol^{-1}
E^0 = effective diffusion coefficient
H_{evp} = evaporation heat of the solid material, J kg^{-1}
H_g = gas enthalpy, J kg^{-1}
H_s = solid-phase enthalpy, J kg^{-1}
h_s = convective mass transfer coefficient between solid and gas, kg m^{-2} s^{-1}
h'_s = convective heat transfer coefficient between solid and gas, W m^{-2} K^{-1}
I_x^+ = radiation flux in positive x direction, W m^{-2}
I_x^- = radiation flux in negative x direction, W m^{-2}
k_a = radiation absorption coefficient, m^{-1}
k_d = rate constants of char burning as a result of diffusion, kg m^{-2} s^{-1}
k_r = rate constants of char burning as a result of chemical kinetics, kg m^{-2} s^{-1}
k_v = rate constant of devolatilization, s^{-1}
k_s = radiation scattering coefficient, m^{-1}
p_g = gas pressure, Pa
Q_h = heat loss/gain of the gases, W m^{-3}
Q_{sh} = thermal source term for solid phase, W m^{-3}
q_r = radiative heat flux, W m^{-2}
R = universal gas constant; process rate, kg m^{-3} s^{-1}
R_{mix} = mixing rate of gaseous phase in the bed, kg m^{-3} s^{-1}
S = stoichiometric coefficients in reactions
S_{sg} = conversion rate from solid to gases arising from evaporation, devolatilization, and char burning, kg m^{-3} s^{-1}

Sy_{ig} = mass sources arising from evaporation, devolatilization, and combustion, kg m^{-3} s^{-1}
Sy_{is} = source term, kg m^{-3} s^{-1}
t = time instant, s
T = temperature, K
U = x-velocity, ms^{-1}
V = y-velocity, ms^{-1}
VM = volatile matter in fuel, wt %
x = coordinate in bed forward-moving direction, m
y = coordinate in bed-height direction, m
Y_{ig} = mass fractions of individual species (such as H_2, H_2O, CO, CO_2, C_mH_n,$\cdots$)
Y_{is} = mass fractions of particle compositions (moisture, volatile, fixed carbon, and ash)

Greek letters

α = molar number of O_2 required to burn unit molar carbon in the char combustion reaction
ε_s = system emissivity
σ_b = Stefan–Boltzmann constant, 5.86×10^{-8} W m^{-2} K^{-4}
υ = remaining volatile in solid at time t
υ_∞ = ultimate yield of volatile
ϕ = void fraction in the bed
λ_g = thermal dispersion coefficient, W m^{-1} K^{-1}
λ_g^0 = effective thermal diffusion coefficient, W m^{-1} K^{-1}
λ_s = effective thermal conductivity of the solid bed, W m^{-1} K^{-1}

Subscripts

C = char gasification
env = environmental
g = gas phase
i = identifier for a component in the solid
m = moisture evaporation
p = particle
s = solid phase
v = volatile release

Literature Cited

1. Swithenbank J. The end of wastes. Annual Lecture for the Institute of Energy, Sheffield University, UK, Nov. 15; 2004.
2. Gort R. *On the Propagation of a Reaction Front in a Packed Bed: Thermal Conversion of Municipal Waste and Biomass*. Academic Dissertation. Enshede, The Netherlands: University of Twente; 1995.
3. Rönnbäck M, Axell M, Gustavsson L, Thunmman H, Leckner B. Combustion processes in a biomass fuel bed—Experimental results. Proc of Progress in Thermochemical Biomass Conversion, Tyrol, Austria; Sep. 17–22; 2000.
4. Friberg R, Blasiak W. Measurements of mass flux and stoichiometry of conversion gas from three different wood fuels as function of volume flux of primary air in packed bed combustion. *Biomass Bioenergy*. 2002;23:189-208.
5. Yang YB, Yamauchi H, Nasserzadeh V, Swithenbank J. Moisture effect on the burning characteristics of simulated MSW on a packed bed. Proc of 4th Int Symp on Waste Treatment Technology, Sheffield, UK, Jun. 29–Jul. 2; 2003.
6. Thunman H, Leckner B. Ignition and propagation of a reaction front in cross-current bed combustion of wet biofuels. *Fuel.* 2001;80:473-481.
7. Saastamoinen JJ, Taipale R, Horttanainen M, Sarkomaa P. Propagation of the ignition front in beds of wood particles. *Combust Flame*. 2000;123:214-226.
8. Peters B. *Thermal Conversion of Solid Fuels*. Southampton, UK: WIT Press; 2003.
9. Yang YB, Nasserzadeh V, Goodfellow J, Goh YR, Swithenbank J. Parameter study on the incineration of municipal solid waste fuels in packed beds. *J Inst Energy*. 2003;75:66-80.
10. Yang YB, Yamauchi H, Nasserzadeh V, Swithenbank J. Effects of fuel devolatilisation on the combustion of wood chips and incineration of simulated municipal solid wastes in a packed bed. *Fuel*. 2003;82:2205-2222.
11. Van der Lans RP, Pedersen LT, Jensen A, Glarborg P, Dam-Johansen K. Modelling and experiments of straw combustion in a grate system. *Biomass Bioenergy*. 2000;19:199-208.
12. Yang YB. Effects of fuel properties on biomass combustion—The latest development. Proc of EPSRC (UK) Annual Scientific Meeting on Supergen Biomass, Biofuel and Energy Crops, Loughborough, UK, Nov. 3–5; 2004.
13. Yang YB, Sharifi VN, Swithenbank J. Effect of air flow rate and fuel moisture on the burning behaviors of biomass and simulated municipal solid wastes in packed beds. *Fuel*. 2004;83:1553-1562.
14. Yang YB, Lim CN, Goodfellow J, Sharifi VN, Swithenbank J. A diffusion model for particle mixing in a packed bed of burning solids. *Fuel*. 2005;84:213-225.
15. Thunman H, Åmand L-E, Ghirelli F, Leckner B. Activity 3.1.3—Modelling and verifying experiments on the whole furnace. *Principles and Models of Solid Fuel Combustion*. PhD Thesis. Göteborg, Sweden: Chalmers University of Technology; 2001.
16. Yang YB, Goh YR, Zakaria R, Nasserzadeh V, Swithenbank J. Mathematical modeling of MSW incineration on a traveling bed. *Waste Manage*. 2002;Vol. 22:pp. 369-380.
17. Yang Y, Goodfellow J, Goh Y, Nasserzadeh V, Swithenbank J. Investigation of channel formation due to random packing in a burning waste bed. *Trans IChemE B*. 2001;79:267-77.
18. Badzioch S, Hawksley PGW, Peter CW. Kinetics of thermal decomposition of pulverized coal particles. *Ind Eng Chem Process Des Dev*. 1970;9:521-530.
19. Siminski VJ, Wright FJ, Edelman RB, Economos C, Fortune OF. *Research on Methods of Improving the Combustion Characteristics of Liquid Hydrocarbon Fuels*. AFAPL TR 72–74. Volumes I and II. Wright Patterson Air Force Base, OH: Air Force Aeropropulsion Laboratory; 1972.
20. Howard JB, William GC, Fine DF. Kinetics of carbon monoxide oxidation in postflame gases. Proc of 14th Int Symp on Combustion. Pittsburgh, PA: The Combustion Institute; 1973:975-986.
21. Hautman AN, Dryer FL, Schlug KP, Glassman I. A multiple-step overall kinetic mechanism for the oxidation of hydrocarbons. *Combust Sci Technol*. 1981;25:219.
22. Arthur JR. Reactions between carbon and oxygen. *Trans Faraday Soc*. 1951;47:167-178.
23. Gray D, Cogoli JG, Essenhigh RH. Problems in pulverised coal and char combustion. *Adv Chem Ser*. 1974;131:72-91.
24. Field MA. Rate of combustion of size-graded fractions of char from a low rank coal between 1200K and 2000K. *Combust Flame*. 1969;13:237-252.
25. Peters B. A detailed model for devolatilisation and combustion of waste material in packed beds. Proc of 3rd Eur Conf on Industrial Furnaces and Boilers (INFUB), Lisbon, Portugal, Apr. 18–21; 1995.
26. Wakao N, Kaguei S. *Heat and Mass Transfer in Packed Beds*. London/New York: Gordon & Breach Science Publishers; 1982.
27. Gosman AD, Lockwood FC. Incorporation of a flux model for radiation into a finite-difference procedure for surface calculations. Proc of 14th Int Symp on Combustion. Pittsburgh, PA: The Combustion Institute; 1972:661-671.
28. Shin D, Choi S. The combustion of simulated waste particles in a bed. *Combust Flame*. 2000;121:167-180.

Manuscript received Feb. 3, 2005, and revision received Jun. 24, 2005.